Electronic Supplementary Information (ESI)

Constructing anion−π interactions in cationic iridium(III) complexes to achieve aggregation−induced emission property

Weilin Song,[a, c]† Jing Gao,[a]† Ying Gao,*[b] Guogang Shan,*[a] Yun Geng,[a] Kuizhan Shao,[a] and Zhong-Min Su*[a, c]

[a] *Institute of Functional Material Chemistry and National & Local United Engineering Lab for Power Battery, Faculty of Chemistry, Northeast Normal University, Changchun, 130024, Jinlin, P. R. China.*

[b] *Jilin Provincial Key Laboratory of Straw Based Functional Materials, Institute for Interdisciplinary Biomass Functional Materials Studies, Jilin Engineering Normal University, Changchun 130052, China.*

[c] *State Key Laboratory of Supramolecular Structure and Materials, Institute of Theoretical Chemistry, College of Chemistry, Jilin University, Changchun 130021, China.*

†These authors contribute equally to this work.

Table of Contents

from S_0 to T_1 as calculated by DFT approach for complexes **Ir-3NMe**, and **Ir-3NPh**.

Experimental Section

1. Materials and instrumentation

If no other special indicated, all reagents and solvents were used as commercially available without further purification. Column chromatographic purification of products was accomplished using 200-300 mesh silica gel. NMR spectra were measured on a Bruker Avance-500 spectrometer in the solvents indicated; chemical shifts are reported in units (ppm) by assigning TMS resonance in the ^1H spectrum as 0.00 ppm, $CDCl_3$ resonance in the ^{13}C spectrum as 77.0 ppm. UV-vis measurements were performed using Cary 500 UV-Vis-NIR. PL spectra for all complexes were measured using FL-4600 FL spectrophotometer. Single crystal X-ray diffraction analysis was carried out on a Bruker Apex CCD II area-detector diffractometer and the structures were refined by SHELXL-97 program.

2. Synthetic procedures

2.1 Synthesis of ligand 2-(3-methyl-5-phenyl-1*H*-pyrazol-1-yl)pyridine **(A1)**

Acetylacetone (10 mmol, 1 g), K_2CO_3 (25 mmol, 3.45 g), tetrabutylammonium bromide (1 mmol, 0.321 g) and 15 mL of water were weighed into a 100 mL double-necked round-bottom flask. Subsequently, CS_2 (12 mmol, 0.73 mL) was added dropwise to the above solvent mixture under stirring conditions. After stirring for 1 h at room temperature, CH_3CH_2I (10 mmol, 0.87 mL) was added slowly dropwise to the reaction solution (note: this process must be slow and the whole dropwise addition process should be kept for more than 15 min), and the obtained mixed solution was stirred at room temperature for 8 h. After the reaction, the precipitate was collected by filtration, and the filter cake was washed repeatedly with water and dried under vacuum to obtain the intermediate, which was a white solid. The white solid (5 mmol, 1.01 g) was weighed and dissolved in 50 mL of dichloromethane and then the reaction solution was cooled to 0º C. After stabilization, H_2SO_4 (20 mmol, 1.1 mL) was added to it dropwise. At the end of the reaction, the reaction mixture was poured into saturated sodium chloride ice water (50 mL) while stirring, and the mixture was neutralized with

aqueous sodium carbonate. After finishing, the organic phase was extracted with dichloromethane and washed with water, dried with anhydrous magnesium sulfate, concentrated under vacuum, and finally purified by column chromatography to obtain pure product **1** in 62% yield. ^{1}H NMR (500 MHz, $CDCl_3$, δ [ppm]): 6.09 (s, 1H), 2.98 (d, J = 34.5 Hz, 4H), 2.19 (s, 3H), 1.36 (s, 6H).

Under nitrogen atmosphere, 5 mL of a mixed solution of THF containing **1** (0.5 mmol, 95 mg), phenylboronic acid (0.75 mmol, 91 mg), $Pd(P(Ph)_3)_4$ (0.0375 mmol, 43 mg) and CuTC (I) (1.0 mmol, 326 mg) was heated to 50ºC for two hours. After cooling to room temperature, the reaction solution was extracted and the filter cake was rinsed with dichloromethane, the collected filtrate was combined and concentrated and purified by column chromatography to give pure product **2** as a yellow oily liquid in 73% yield. ^{1}H NMR (500 MHz, $CDCl_3$, δ [ppm]): 7.31-7.33 (m, 4H), 7.23-7.35 (m, 1H), 5.99 (s, 1H), 2.70-2.75 (m, 2H), 1.70 (s, 3H), 1.24-1.27 (m, 3H).

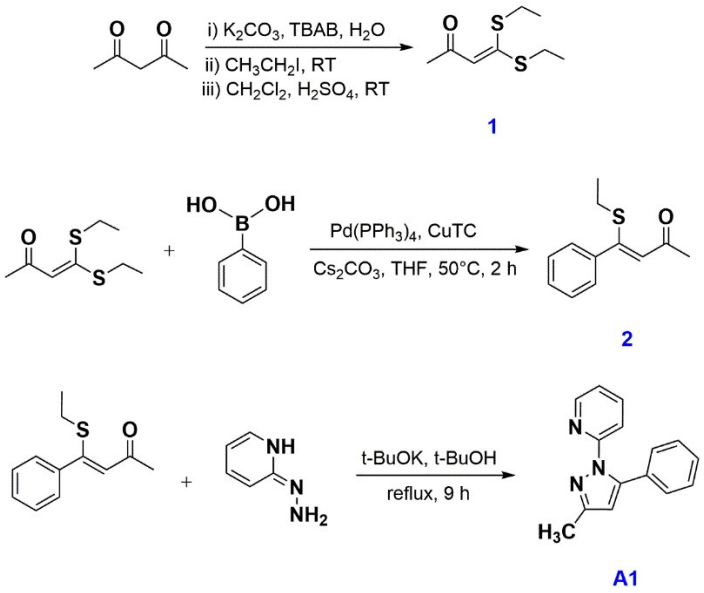

Scheme S1 Synthetic routes of **A1**.

Finally, weighed **2** (0.5 mmol, 103 mg), 2-hydrazinopyridine (0.6 mmol, 65 mg), potassium tert-butoxide (1.0 mmol, 112 mg) and 5 mL of tert-butanol were placed in a round bottom flask and the whole reaction was heated to reflux and stirred for 9 h. After cooling to room temperature, the reaction solution was extracted and the filter cake was rinsed with dichloromethane, the collected filtrate was combined and concentrated to

obtain pure product **A1** as a white solid by column chromatography, and the synthesis procedure was shown in **Scheme S1** with a yield of 58%. ^{1}H NMR (500 MHz, $CDCl_3$, δ [ppm]): 8.38-8.40 (m, 1H), 7.66-7.70 (m, 1H), 7.29-7.33 (m, 4H), 7.23-7.26 (m, 2H), 7.16-7.18 (m, 1H), 6.32 (s, 1H), 2.40 (s, 3H).

2.2 Synthesis of ligand 2-(3,5-diphenyl-1*H*-pyrazol-1-yl)pyridine **(A2)**

$Co(OAc)_2 \cdot H_2O$ (3.75 g, 0.15 mmol) and CrO_3 (3.0 g, 0.03 mmol) were taken in a two-neck flask under argon atmosphere with 100 mL of distilled water. After the mixture was heated to 60°C, 4.5 mL pyridine was added slowly via a constant pressure dropping funnel. The mixture kept at this temperature for stirring 10 min. The target product **TPCD** was washed with acetone and collected by filtration.

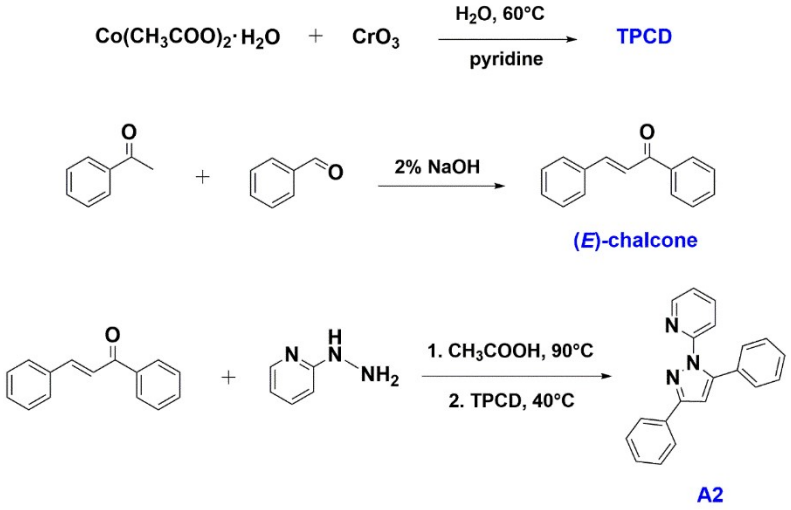

Scheme S2 Synthetic routes of **A2**.

Benzaldehyde (4.7 g, 50 mmol) and acetophenone (6.0 g 50 mmol) were added into a 250 mL round-bottomed flask with a reflux condenser. Subsequently, NaOH aqueous solution (15 mL, 2%) was added dropwise to the above solution under vigorous magnetic stirring. The resulting mixture was agitated for 30 min, and then treated at 60°C for 6 h using an oil bath. After cooling to room temperature, the precipitate was filtrated and washed with distilled water, intermediate product (*E*)-chalcone was obtained. 2-Hydrazinopyridine (1.1g 10 mmol) was dropwise added to a 100 mL three-necked flask charged with (*E*)-chalcone (2.08 g, 10 mmol) in glacial acetic acid. The reaction mixture was heated to 90°C for 2 h. After this time, TPCD (2.4 g, 4 mmol) was added and stirred at 40°C for 2 h. After cooling, the solution was poured into water, and

the solid residue was filtered, washed with 5% HCl and water. The crude product **A2** was purified by column chromatography with petroleum ether/ethyl acetate (10/1) to give a white solid. (Yield 60.9%) ^{1}H NMR (500 MHz, $CDCl_3$, δ [ppm]): 8.37-8.38 (m, 1H), 7.93-7.95 (m, 2H), 7.74-7.78 (m, 1H), 7.57 (d, J = 8.0 Hz, 1H), 7.43 (t, J = 7.5 Hz, 2H), 7.30-7.36 (m, 6H), 7.19~7.22 (m, 1H), 6.83 (s, 1H).

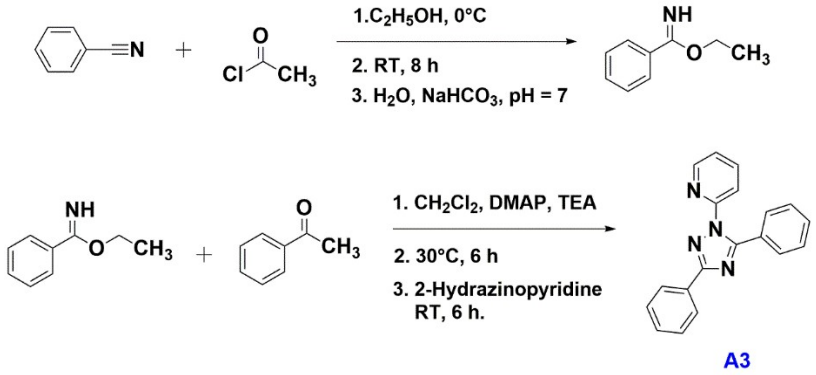

Scheme S3 Synthetic routes of **A3**.

2.3 Synthesis of ligand 2-(3,5-diphenyl-1*H*-1,2,4-triazol-1-yl)pyridine (**A3)**

Benzonitrile (10.3 g, 100 mmol) was taken in 70 mL of ethanol in a 250 mL round-bottomed flask. Then acetyl chloride (62.8 g, 800 mmol) was added dropwise at 0°C. After dripping, it was raised to room temperature and reacted for 8 hours. Then, the reaction solution was concentrated under reduced pressure to remove excess acetyl chloride and ethanol. The solid residue was dissolved in 100 mL water. Then, the mixture was neutralized with saturated $NaHCO_3$ solution to neutrality and extracted with ether. The organic layer was dried over anhydrous $MgSO_4$, and the solvent was evaporated under reduced pressure to form an intermediate complex ethyl benzimidate. Cool to 0°C, benzoyl chloride (5.62 g, 40 mmol), triethylamine (4.44 g, 44 mmol) and acylation catalyst 4-dimethylaminopyridine (DMAP, 0.49 g, 40 mmol) were added by dripping it into a solution of the ethyl benzimidate (5.96 g, 40 mmol) dissolved in 150 mL dichloromethane. After dripping, the reaction temperature was raised to 30°C for 6 h and then cooled to room temperature. Subsequently, 2-hydrazine pyridine (4.37 g, 40 mmol) was added dropwise. After reacting for 6 h at room temperature, the mixture was extracted with dichloromethane and dried over anhydrous Na_2SO_4. The solvent was removed under reduced pressure and the crude product was purified by

chromatography

with petroleum ether/ethyl acetate (5/1) to give the desired product **A3**. (Yield 50%) ^{1}H NMR (500 MHz, $CDCl_3$, δ [ppm]): 8.33-8.35 (m, 1H), 8.27-8.29 (m, 2H), 7.67-7.71 (m, 1H), 7.52-7.57 (m, 3H), 7.41-7.45 (m, 2H), 7.28-7.39 (m, 4H), 7.17-7.19 (m, 1H).

2.4 Synthesis of ligand 2-(3-methyl-5-phenyl-1*H*-1,2,4-triazol-1-yl)pyridine **(A4)**

Compound **A4** was synthesized in a manner similar to that used for **A3**, where benzonitrile was replaced with acetonitrile. (Yield 20%) ^{1}H NMR (500 MHz, CDCl3, δ [ppm]): 8.45-8.47 (m, 1H), 7.80-7.83 (m, 1H), 7.49-7.52 (m, 2H), 7.45-7.47 (m, 1H), 7.39-7.43 (m, 1H), 7.32-7.37 (m, 3H), 2.53 (s, 3H).

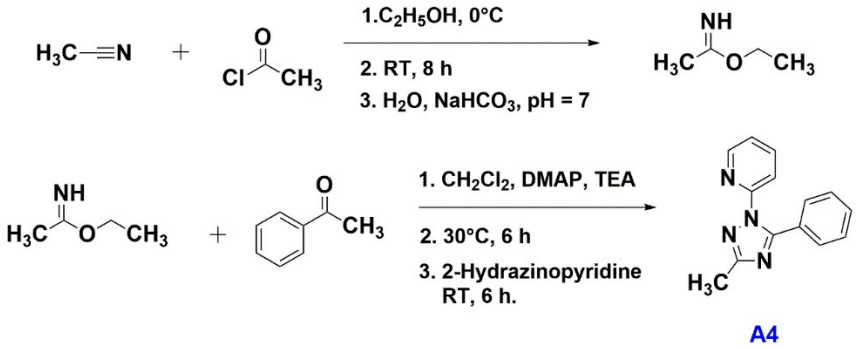

Scheme S4 Synthetic routes of **A4**.

2.5 General procedure for the synthesis of complexes

Four cationic iridium(III) complexes **Ir-2NMe**, **Ir-2NPh**, **Ir-3NMe**, and **Ir-3NPh** were synthesized according to previously reported procedures. The synthetic routes, including the structures of both complexes, were shown in **Scheme S5**. The prior synthesized chloro-bridge di-iridium intermediatecomplex **[(dfppz)$_2$Ir(*μ*-Cl)]$_2$** and the respective ancillary N^N ligand were transferred into a round-bottomed flask. Ethylene glycol was added and the reaction mixture was heated at 150 °C for 24 h, to give a clear solution. After cooling to room temperature, an ion exchange reaction with aqueous solution of NH_4PF_6 (0.163 mg, 1.0 mmol) was carried out to afford the luminescent iridium complexes in high yields. The resulting product was chromatographed on silica gel and crystallized to obtain the desired purified complexes.

Synthesis of **Ir-2NMe**: **[(dfppz)$_2$Ir(*μ*-Cl)]$_2$** (1.0 g, 0.85 mmol), **A1** (0.4 g, 1.7 mmol), ethylene glycol (30 mL). Yellowish green powder (yield: 76%). ^{1}H NMR (500 MHz,

d_6-DMSO, δ [ppm]): 8.69 (d, J = 3.0 Hz, 2H), 7.94-8.06 (m, 1H), 7.82-7.83 (m, 1H), 7.71 (d, J = 2.0 Hz, 1H), 7.63-7.68 (m, 6H), 7.40 (t, J = 6.5 Hz, 1H), 7.13-7.18 (m, 1H), 7.07-7.11 (m, 1H), 7.03 (d, J = 9.0 Hz, 1H), 6.86-6.88 (m, 2H), 6.83 (s, 1H), 5.56-5.66 (m, 2H), 1.83 (s, 3H). ^{13}C NMR (125 MHz, d_6-DMSO, δ [ppm]): 162.7, 160.9, 160.8, 160.6, 160.5, 158.9, 158.8, 158.6, 158.5, 156.6, 150.5, 150.0, 149.9, 149.8, 148.1, 148.0, 147. 9, 147.8, 141.7, 140.8, 140.2, 136.4, 136.3, 135.3, 135.2, 133.1, 133.0, 132.9, 131.4, 131.0, 129.7, 128.7, 127.49, 127.45, 127.4, 125.0, 115.6, 115.4, 114.93, 114.89, 114.7, 114.4, 110.2, 110.0, 100.6, 100.4, 100.3, 100.1, 99.9, 99.74, 99.70, 99.5, 13.8. MS (MALDI-TOF, m/z): 786.2147 $[M]^+$.

Synthesis of **Ir-2NPh**: **$[(dfppz)_2Ir(\mu\text{-}Cl)]_2$** (0.8 g, 0.68 mmol), **A2** (0.4 g, 1.3 mmol), ethylene glycol (30 mL). Pale yellow powder (yield: 73%). ^{1}H NMR (500 MHz, d_6-DMSO, δ [ppm]): 8.65 (d, J = 2.5 Hz, 1H), 8.61 (d, J = 2.5 Hz, 1H), 8.05-8.08 (m, 1H), 7.89-7.90 (m, 1H), 7.74 (t, J = 2.5 Hz, 2H), 7.64-7.71 (m, 5H), 7.47-7.50 (m, 1H), 7.19-7.22 (m, 2H), 7.13-7.17 (m, 1H), 7.07-7.11 (m, 3H), 6.99-7.00 (m, 2H), 6.89 (t, J = 2.7 Hz, 2H), 6.59-6.64 (m, 1H), 6.55-6.57 (m, 1H), 4.96-4.98 (m, 1H). ^{13}C NMR (125 MHz, d_6-DMSO, δ [ppm]): 160.7, 160.6, 160.2, 160.1, 159.2, 158.7, 158.6, 158.2, 158.1, 150.2, 149.9, 149.8, 149.7, 149.2, 149.1, 148.5, 147.8, 147.7, 147.2, 147.1, 141.7, 140.4, 140.3, 135.84, 135.79, 134.61, 134.56, 133.1, 133.0, 132.7, 132.5, 131.5, 130.2, 130.1, 129.8, 129.0, 128.5, 128.3, 128.1, 127.50, 127.47, 126.93, 126.89, 125.7, 116.5, 115.2, 115.0, 114.9, 113.9, 110.5, 110.0, 100.5, 100.3, 100.1, 99.2, 99.0, 98.8. MS (MALDI-TOF, m/z): 848.2349 $[M]^+$.

Synthesis of **Ir-3NMe**: **$[(dfppz)_2Ir(\mu\text{-}Cl)]_2$** (1.0 g, 0.85 mmol), **A4** (0.42 g, 1.8 mmol), ethylene glycol (30 mL), Yellowish green powder (yield: 66%). ^{1}H NMR (500 MHz, d_6-DMSO, δ [ppm]): 8.69 (t, J = 2.7 Hz, 2H), 8.10-8.14 (m, 1H), 7.95 (d, J = 2.5 Hz, 1H), 7.84-7.87 (m, 3H), 7.75-7.79 (m, 1H), 7.69-7.72 (m, 2H), 7.66 (d, J = 2.5 Hz, 1H), 7.49-7.52 (m, 1H), 7.29 (d, J = 8.5 Hz, 1H), 7.09-7.20 (m, 2H), 6.87-6.89 (m, 2H), 5.61-5.63 (m, 1H), 5.55-5.57 (m, 1H), 1.97 (s, 3H). ^{13}C NMR (125 MHz, d_6-DMSO, δ [ppm]): 164.2, 160.8, 160.6, 160.5, 158.8, 158.7, 158.6, 158.4, 150.3, 149.9, 148.6, 147.9, 142.2, 141.4, 140.6, 135.5, 135.4, 134.0, 133.9, 133.2, 133.1, 132.8, 130.0,

129.9, 127.5, 127.3, 126.4, 115.6, 115.4, 114.9, 114.7, 110.1, 100.7, 100.5, 100.3, 100.1, 99.8, 13.7. MS (MALDI-TOF, m/z): 787.2142 $[M]^+$.

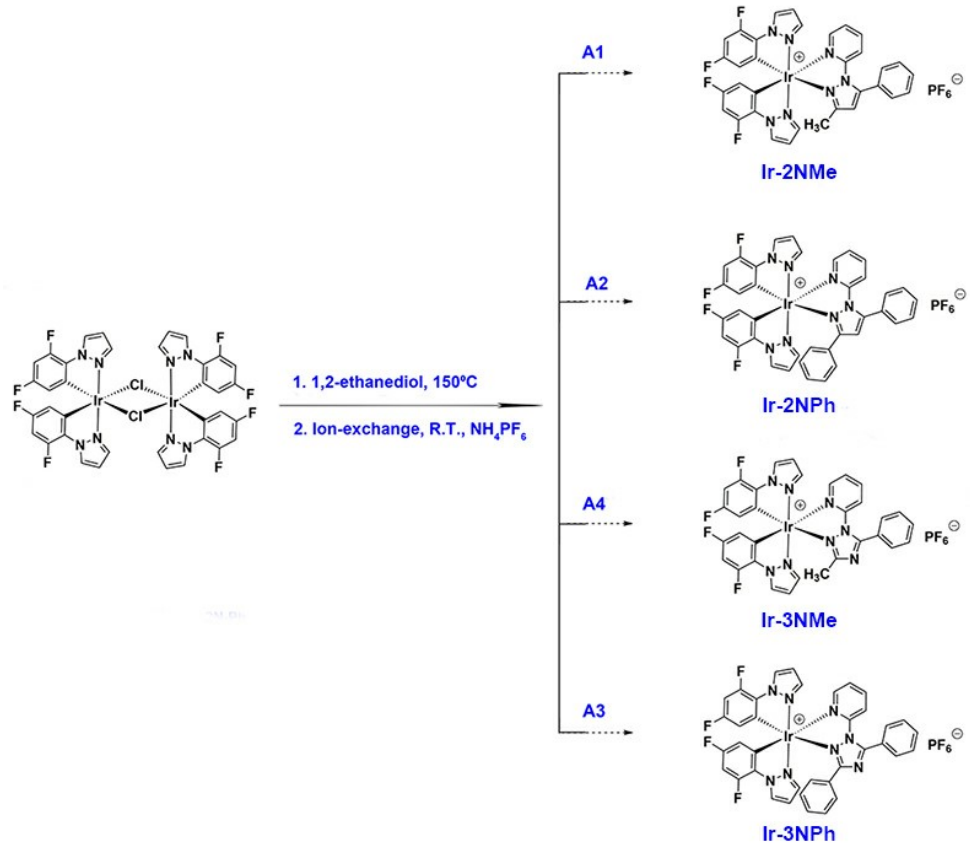

Scheme S5 Synthetic routes of complexes **Ir-2NMe**, **Ir-2NPh**, **Ir-3NMe**, and **Ir-3NPh**.

Synthesis of **Ir-3NPh**: **$[(dfppz)_2Ir(\mu\text{-}Cl)]_2$** (0.8 g, 0.68 mmol), **A3** (0.43 g, 1.4 mmol), Pale yellow powder (yield: 69%). ^{1}H NMR (500 MHz, d_6-DMSO, δ [ppm]): 8.70 (d, J = 3.0 Hz, 1H), 8.52 (d, J = 3.0 Hz, 1H), 8.16-8.20 (m, 1H), 8.10 (d, J = 3.0 Hz, 1H), 7.92-7.95 (m, 3H), 7.88-7.89 (m, 1H), 7.79-7.82 (m, 1H), 7.73 (t, J = 7.5 Hz, 2H), 7.56-7.59 (m, 1H), 7.44 (d, J = 8.5 Hz, 1H), 7.31-7.35 (m, 1H), 7.22-7.24 (m, 2H), 7.12-7.17 (m, 3H), 6.93 (t, J = 2.7 Hz, 1H), 6.86 (t, J = 2.7 Hz, 1H), 7.66-7.71 (m, 1H), 5.61-5.63 (m, 1H), 5.20-5.22 (m, 1H). ^{13}C NMR (125 MHz, d_6-DMSO, δ [ppm]): 165.7, 160.6, 160.5, 160.3, 160.2, 158.6. 158.5, 158.3, 158.2, 150.2, 150.0, 149.8, 149.2, 149.1, 148.4, 147.9, 147.8, 147.1, 147.0, 142.2, 141.2, 140.6, 137.0, 135.0, 134.95, 133.6, 133.5, 133.2, 133.1, 132.7, 132.6, 131.2, 130.1, 130.0, 129.3, 128.9, 128.1, 127.5,

127.0, 126.9, 126.8, 126.7, 125.8, 117. 0, 115.7, 115.5, 115.2, 115.0, 110.4, 110.0, 100.7, 100.6, 100.5, 100.3, 99.6, 99.4, 99.2. MS (MALDI-TOF, m/z): 849.2332 $[M]^+$.

2.6 Single Crystal X-Ray Diffraction Analysis

Single crystal of complexes **Ir-2NMe**, **Ir-2NPh**, **Ir-3NMe**, and **Ir-3NPh** were obtained by solvent diffusion method (from ethyl ether to dichloromethane). The crystals were mounted on glass fiber and the data were collected on a on a Bruker Apex CCD II area-detector diffractometer. The structure was solved with the ShelXT structure solution program using the Intrinsic Phasing solution method and by using Olex2 as the graphical interface. Further details of the crystal structure determination have been deposited to the Cambridge Crystallographic Data Centre as supplementary publication. CCDC 2171675 (**Ir-2NMe**), 2171672 (**Ir-2NPh)**, 2171674 (**Ir-3NMe**), and 2171673 (**Ir-3NPh**) contain the supplementary crystallographic data for this paper.

2.7 Computational Details

The Gaussian 09 program was utilized to perform DFT calculations. The optimized geometries and electron configurations were investigated using the density functional theory (DFT) and time-dependent DFT (TDDFT) with no symmetry constraints at the B3LYP level. The ground-state structures were optimized based on their corrspoding single crystal structures. The LANL2DZ basis set was used to treat the Ir atom, whereas the 6-31G** basis set was used to treat C, H, O, N, and F atoms. Solvent effects were considered within the SCRF (self-consistent reaction field) theory to model the interaction with the solvent (CH_3CN). The anion−π interaction energies were calculated by single point calculation using the DFT method according to the equation $E = E_{complex} - E_{anion} - E_{cation}$, where E = anion−π interaction energy, $E_{complex}$ = the energy of complexes **Ir-2NMe**, **Ir-2NPh**, **Ir-3NMe**, or **Ir-3NPh**, E_{anion} = the energy of anion, E_{cation} = the energy of cation.

2.8 Electrochemical characterization

Cyclic voltammetry was performed on an electrochemical workstation (BAS100W instrument) in CH_3CN solutions (1×10^{-3} M) at a scan rate of 100 mV s^{-1} using a glassy-carbon electrode as the working electrode, an aqueous saturated calomel electrode as

the reference electrode, and a platinum-wire electrode as the auxiliary electrode. Tetrabutylammonium hexafluorophosphate (1×10^{-1} M) and ferrocene was selected as the supporting electrolyte and internal standard, respectively.

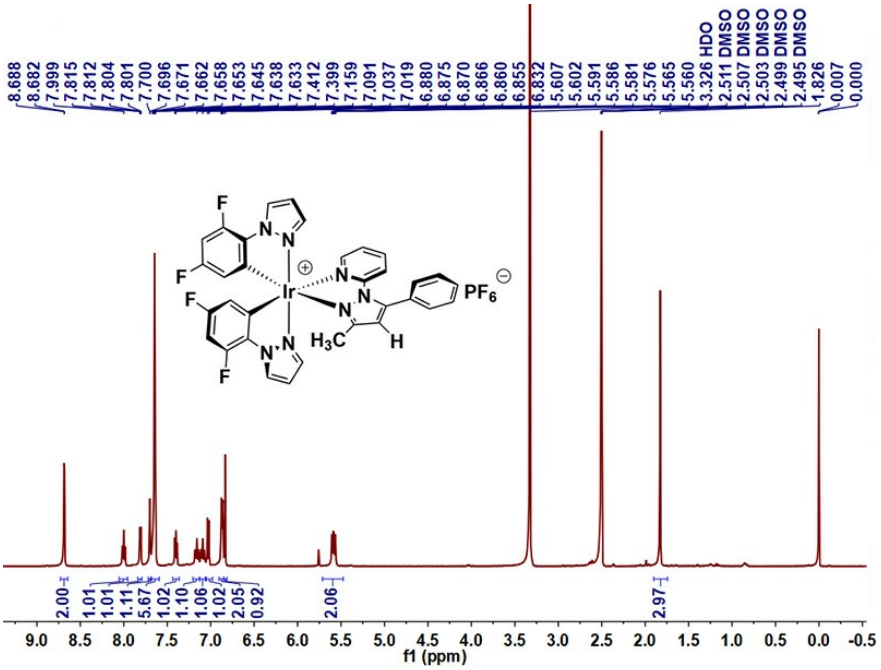

Fig. **S1** ^{1}H NMR spectrum of **Ir-2NMe** in *d6*-DMSO.

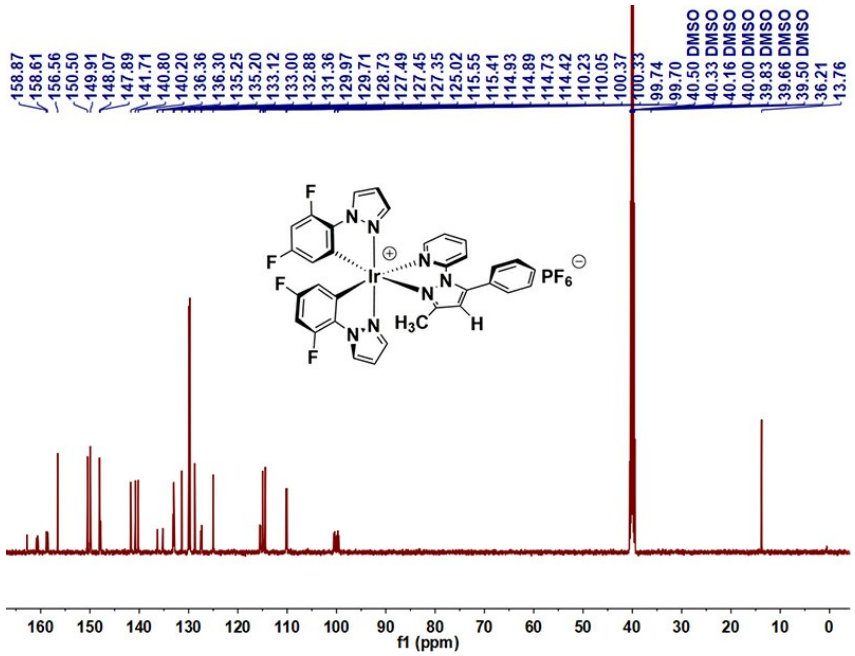

Fig. **S2** ^{13}C NMR spectrum of **Ir-2NMe** in *d6*-DMSO.

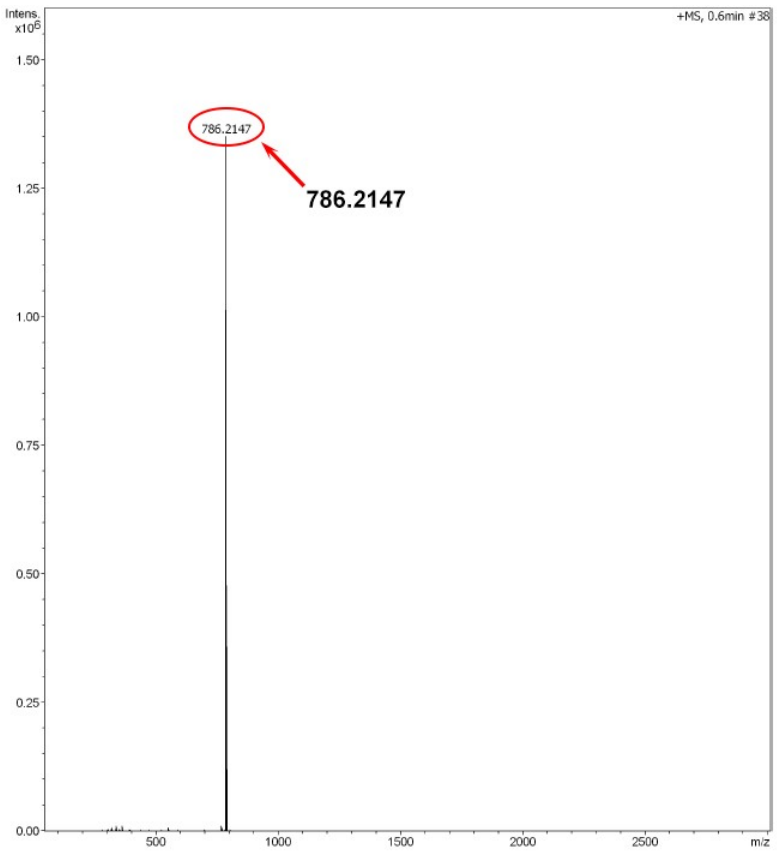

Fig. **S3** Copy of the MALDI-TOF MS spectrum for **Ir-2NMe** (positive mode).

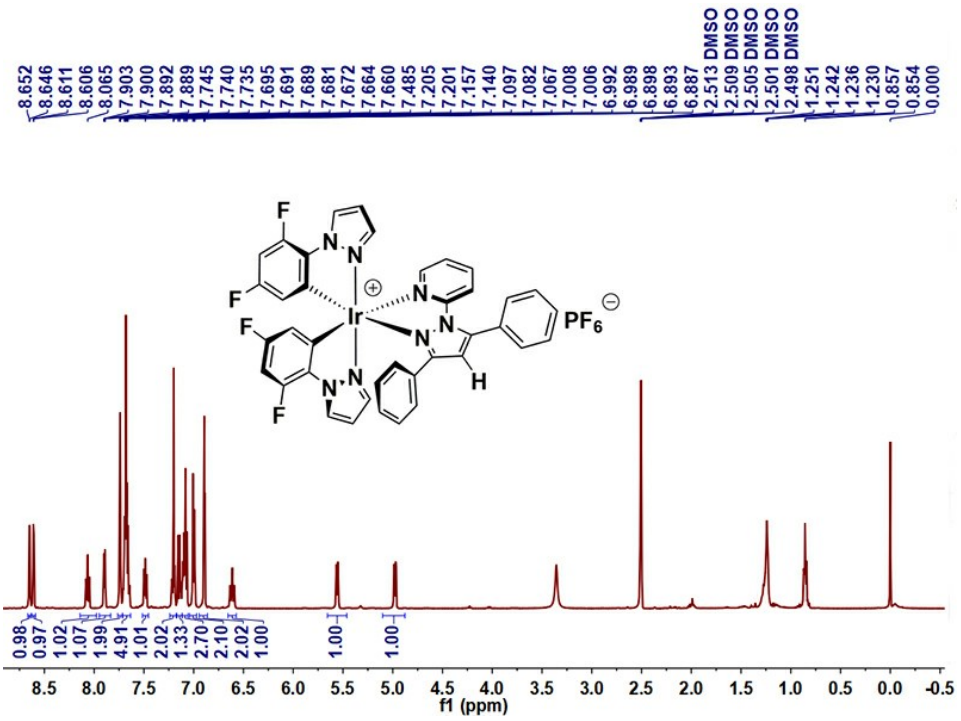

Fig. **S4** ^{1}H NMR spectrum of **Ir-2NPh** in *d6*-DMSO.

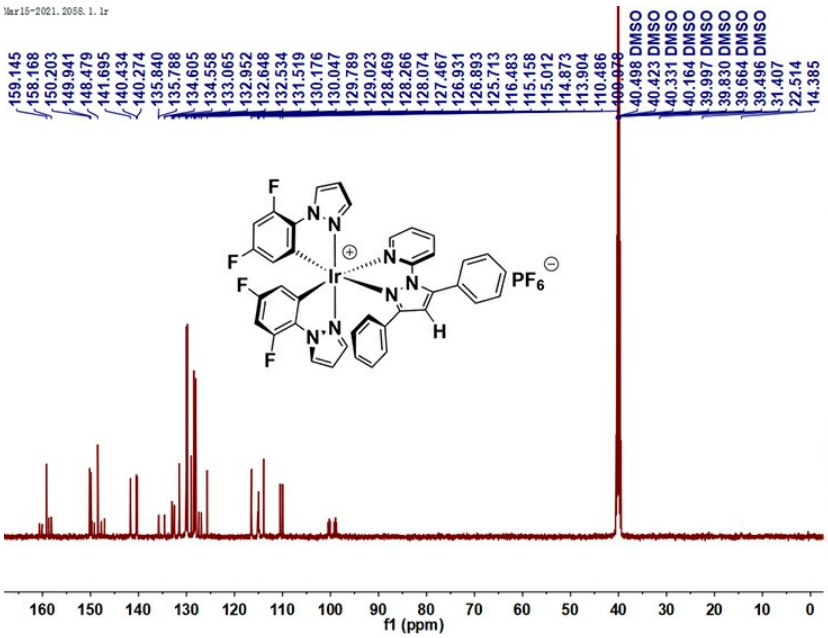

Fig. **S5** ^{13}C NMR spectrum of **Ir-2NPh** in *d6*-DMSO.

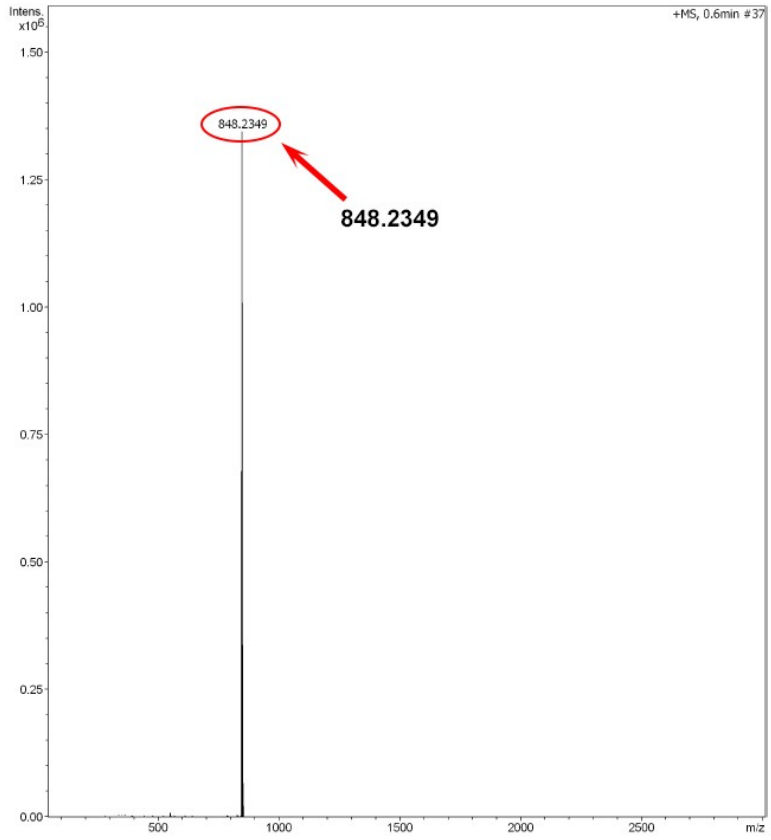

Fig. **S6** Copy of the MALDI-TOF MS spectrum for **Ir-2NPh** (positive mode).

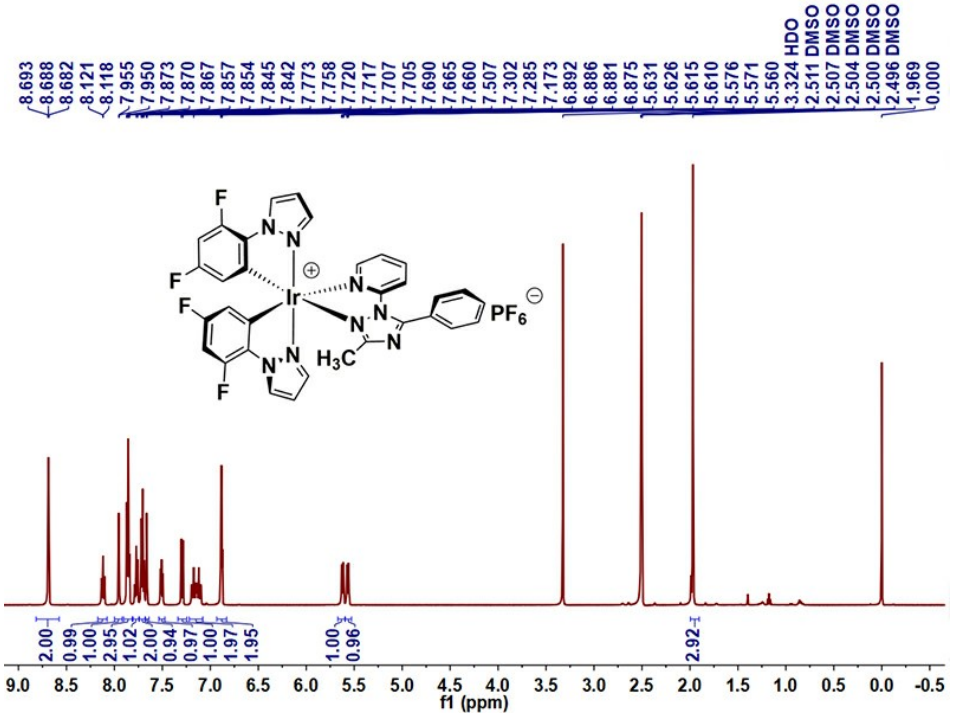

Fig. **S7** ^{1}H NMR spectrum of **Ir-3NMe** in *d*$_6$-DMSO.

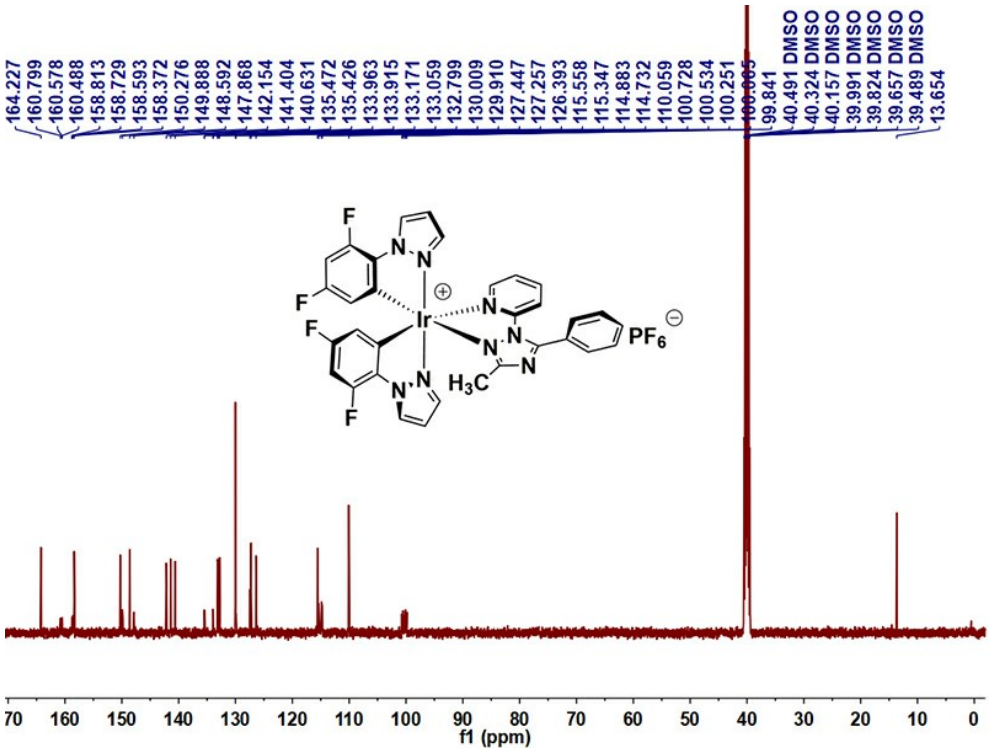

Fig. **S8** ^{13}C NMR spectrum of **Ir-3NMe** in *d*$_6$-DMSO.

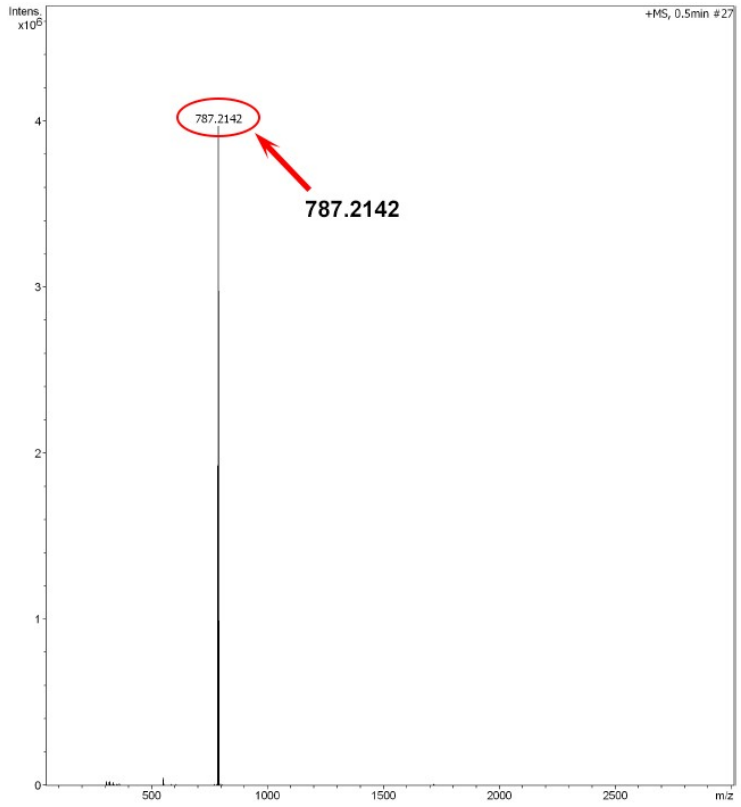

Fig. **S9** Copy of the MALDI-TOF MS spectrum for **Ir-3NMe** (positive mode).

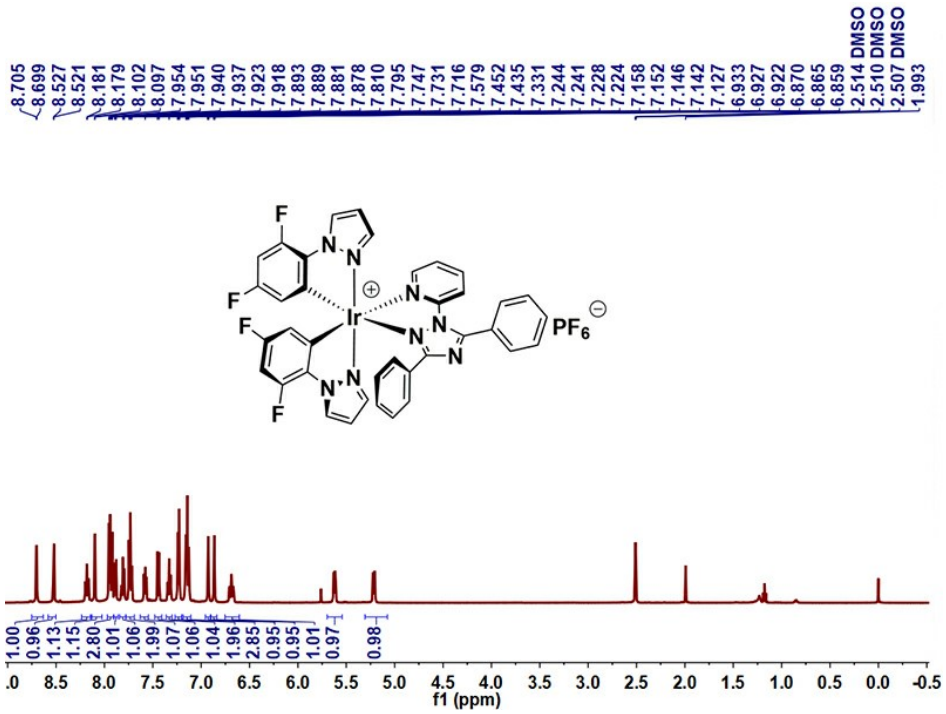

Fig. **S10** ^{1}H NMR spectrum of **Ir-3NPh** in *d6*-DMSO.

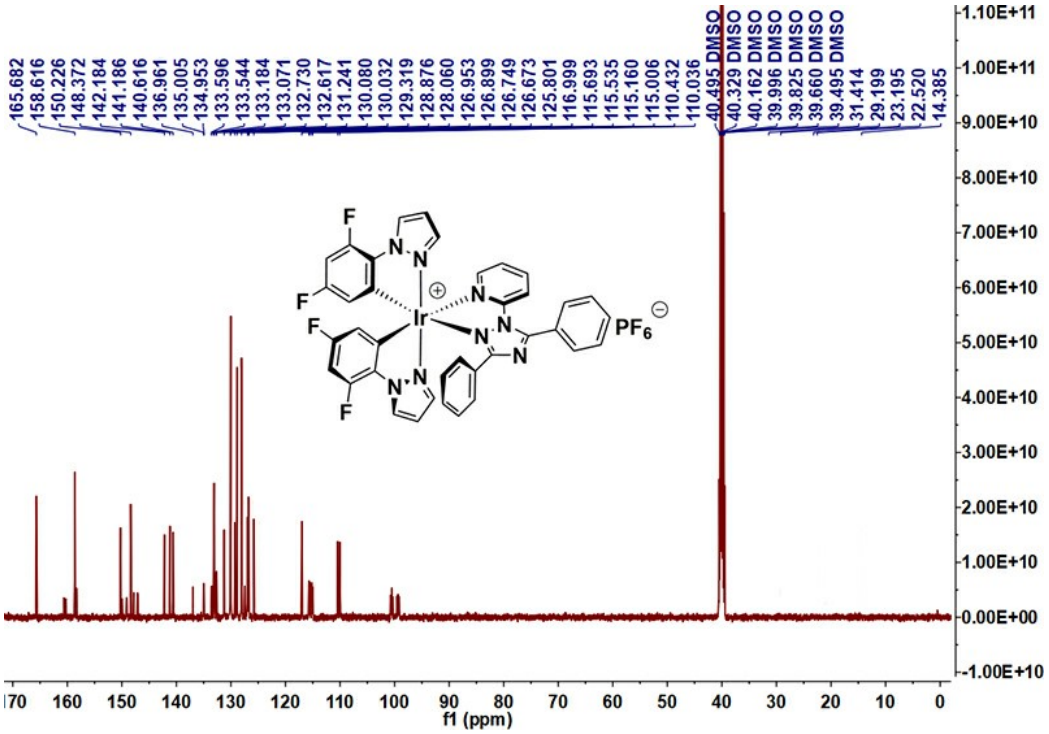

Fig. **S11** ^{13}C NMR spectrum of **Ir-3NPh** in *d6*-DMSO.

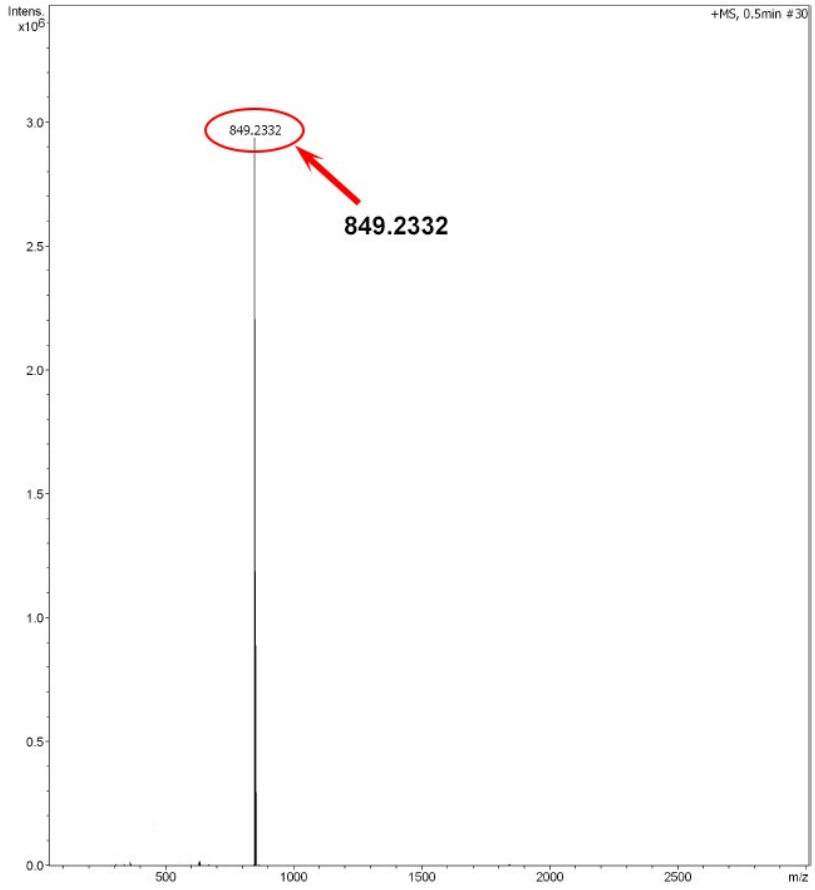

Fig. **S12** Copy of the MALDI-TOF MS spectrum for **Ir-3NPh** (positive mode).

Table S1 Crystal data and structure refinement for complexes **Ir-2NMe**, **Ir-2NPh**, **Ir-3NMe**, and **Ir-3NPh**.

Complexes	**Ir-2NMe**	**Ir-2NPh**	**Ir-3NMe**	**Ir-3NPh**
CCDC	2171675	2171672	2171674	2171673
Empirical formula	$C_{33}H_{23}F_{10}IrN_7P$	$C_{38}H_{25}F_{10}IrN_7P$	$C_{32}H_{22}F_{10}IrN_8P$	C37H24F10IrN8P
Formula weight	930.75	992.82	931.74	993.81
Temperature (K)	290.56	273.15	293(2)	295.15
Crystal system	monoclinic	orthorhombic	tetragonal	orthorhombic
space group	C2/c	$P2_12_12_1$	$I4_1cd$	$P2_12_12_1$
a/Å	20.520(6)	10.2757(13)	18.5579(18)	10.2934(19)
b/Å	29.923(8)	16.345(2)	18.5579(18)	16.296(3)
c/Å	13.743(4)	24.332(3)	42.424(8)	24.178(5)
α /°	90	90	90	90
β /°	116.583(10)	90	90	90
γ /°	90	90	90	90
V/Å^3	7547(4)	4086.7(9)	14611(4)	4055.6(13)
Z	8	4	16	4
ρ calc (g/cm^3)	1.638	1614	1.694	1.628
μ/mm^{-1}	3.663	7.429	8.272	7.494
R_{int}	0.0538	0.0546	0.0465	0.0466
Goodness of fit on F^2	1.189	1.028	1.088	1.038
R_1[a], wR_2[b][I>2σ(I)]	0.0818, 0.2038	0.0329, 0.0770	0.0310, 0.0795	0.0365, 0.0844
R_1, wR_2 (all data)	0.0949, 0.2167	0.0372, 0.0786	0.0317, 0.0799	0.0409, 0.0866

[a] $R_1 = \Sigma||Fo|-|Fc||/\Sigma|Fo|$. [b] $wR_2 = \{\Sigma[w(Fo^2-Fc^2)^2]/\Sigma[w(Fo^2)^2]\}^{1/2}$

Table S2 Selected bond lengths (Å) for complexes **Ir-2NMe**, **Ir-2NPh**, **Ir-3NMe**, and **Ir-3NPh**.

Complexes	**Ir-2NMe**	**Ir-2NPh**	**Ir-3NMe**	**Ir-3NPh**
Ir-$N_{cyclometalated\text{-}ligands}$	1.984 Å	2.012 Å	2.019 Å	2.002 Å
Ir-$N_{cyclometalated\text{-}ligands}$	1.997 Å	2.020 Å	2.020 Å	2.007 Å
Ir-$N_{ancillary\text{-}ligand}$	2.067 Å	2.134 Å	2.134 Å	2.143 Å
Ir-$N_{ancillary\text{-}ligand}$	2.118 Å	2.158 Å	2.140 Å	2.161 Å

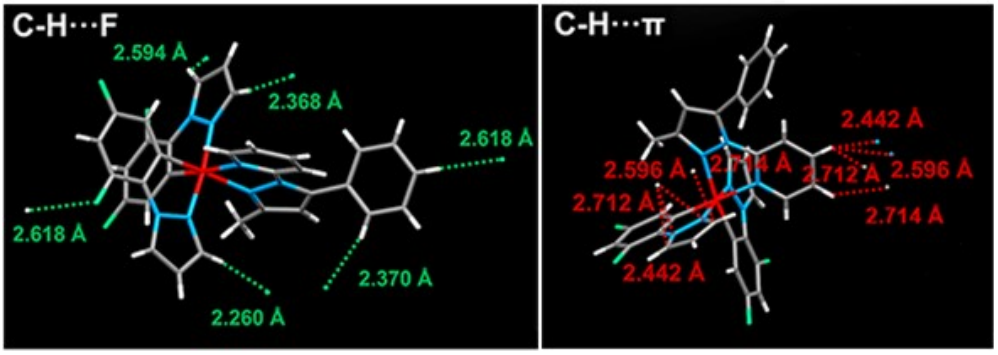

Fig. **S13** Intramolecular interactions of complex **Ir-2NMe**.

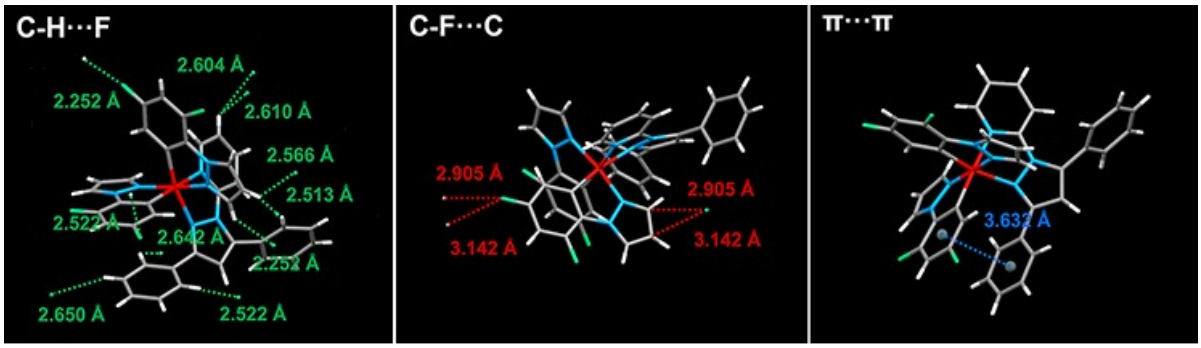

Fig. **S14** Intramolecular interactions of complex **Ir-2NPh**.

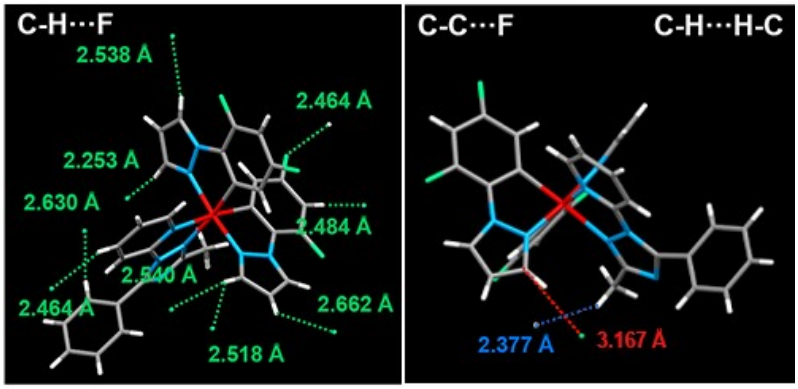

Fig. **S15** Intramolecular interactions of complex **Ir-3NMe**.

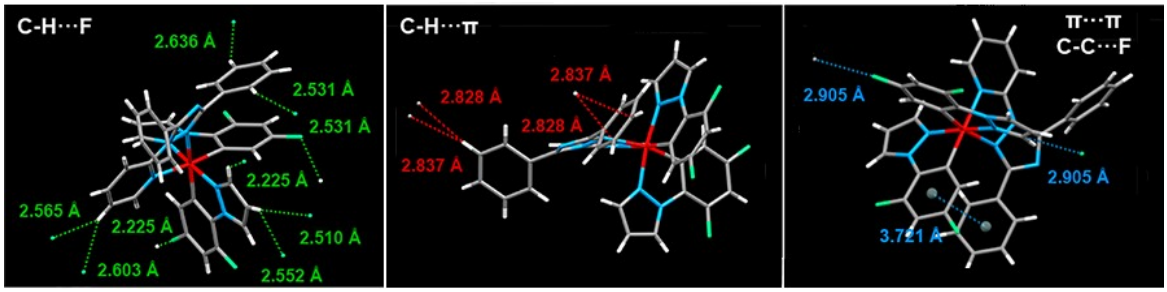

Fig. **S16** Intramolecular interactions of complex **Ir-3NPh**.

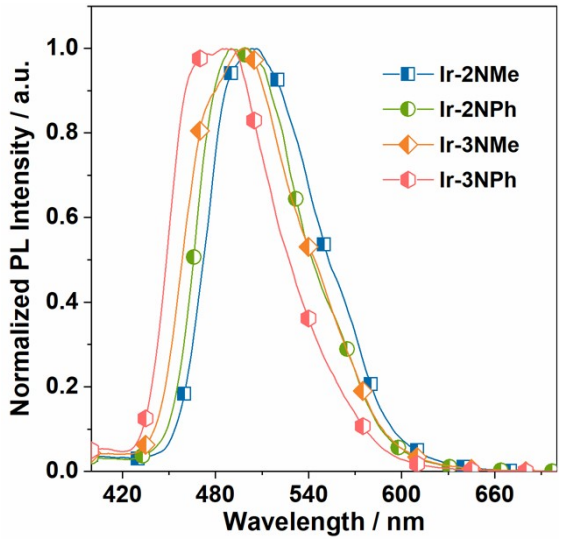

Fig. **S17** PL spectra of iridium(III) complexes in CH_3CN (10^{-5} M) at 77 K.

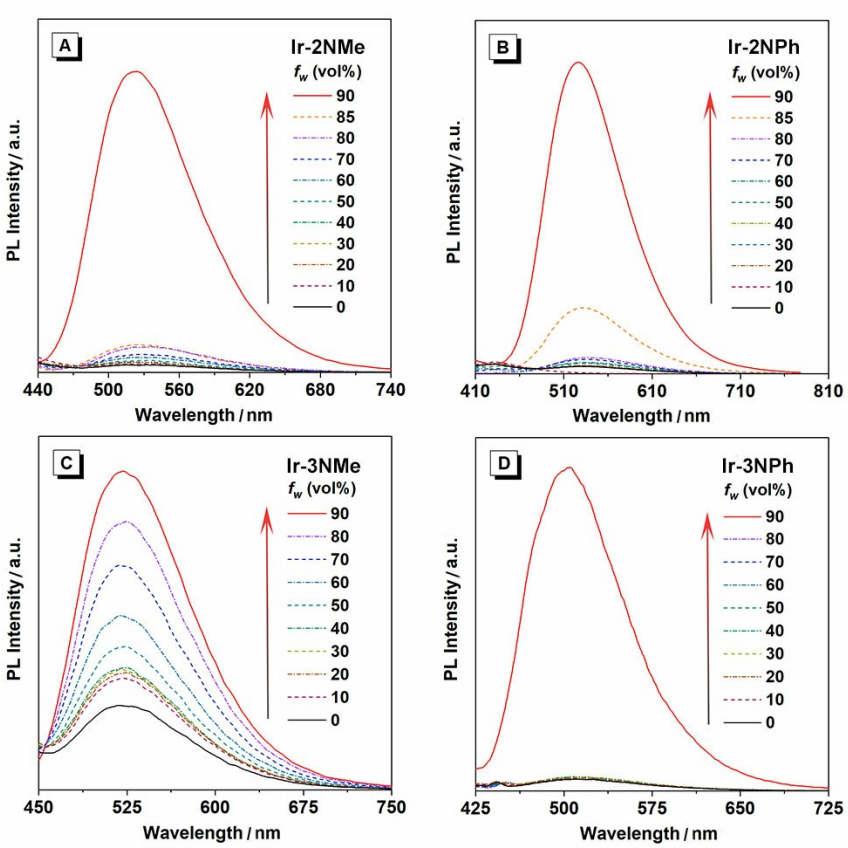

Fig. **S18** Emission spectra of complexes, in CH_3CN-water mixtures with different water fractions (0-90%).

Table S3 Intermolecular interactions statistics of the complexes **Ir-2NMe**, **Ir-2NPh**, **Ir-3NMe**, and **Ir-3NPh**.

Ir-2NMe		**Ir-2NPh**		**Ir-3NMe**		**Ir-3NPh**	
Type of bonds	Distance (Å)	Type of bonds	Distance (Å)	Type of bonds	Distance (Å)	Type of bonds	Distance (Å)
Anion···π	3.440	Anion···π	3.288	Anion···π	3.156	Anion···π	3.195
Anion···π	3.663	Anion···π	3.457	Anion···π	3.423	Anion···π	3.421
Anion···π	3.843	Anion···π	3.581	Anion···π	3.663	Anion···π	3.559
Anion···π	3.154	Anion···π	3.767	Anion···π	3.674	Anion···π	3.647
Anion···π	4.001	C-H···F	2.252	C-H···F	2.253	C-H···F	2.225
C-H···F	2.260	C-H···F	2.252	C-H···F	2.464	C-H···F	2.225
C-H···F	2.368	C-H···F	2.513	C-H···F	2.464	C-H···F	2.510

C-H···F	2.370	C-H···F	2.522	C-H···F	2.484	C-H···F	2.531
C-H···F	2.594	C-H···F	2.522	C-H···F	2.518	C-H···F	2.531
C-H···F	2.618	C-H···F	2.566	C-H···F	2.538	C-H···F	2.552
C-H···F	2.618	C-H···F	2.604	C-H···F	2.540	C-H···F	2.565
C-H···π	2.442	C-H···F	2.610	C-H···F	2.630	C-H···F	2.603
C-H···π	2.442	C-H···F	2.642	C-H···F	2.662	C-H···F	2.636
C-H···π	2.596	C-H···F	2.650	C-C···F	3.167	C-H···π	2.828
C-H···π	2.596	C-F···C	2.905	C-H···H-C	2.377	C-H···π	2.828
C-H···π	2.712	C-F···C	2.905			C-H···π	2.837
C-H···π	2.712	C-F···C	3.142			C-H···π	2.837
C-H···π	2.714	C-F···C	3.142			C-C···F	2.905
C-H···π	2.714	π···π	3.632			C-C···F	2.905
						π···π	3.721

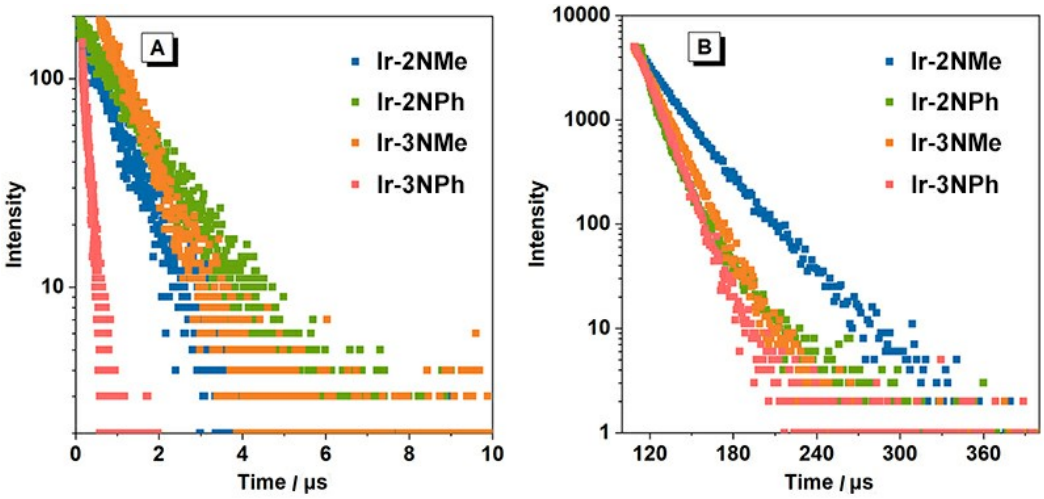

Fig. **S19** Emission lifetime decay curves of complexes **Ir-2NMe**, **Ir-2NPh**, **Ir-3NMe**, and **Ir-3NPh** recorded A) in CH_3CN solution and B) in the solid state.

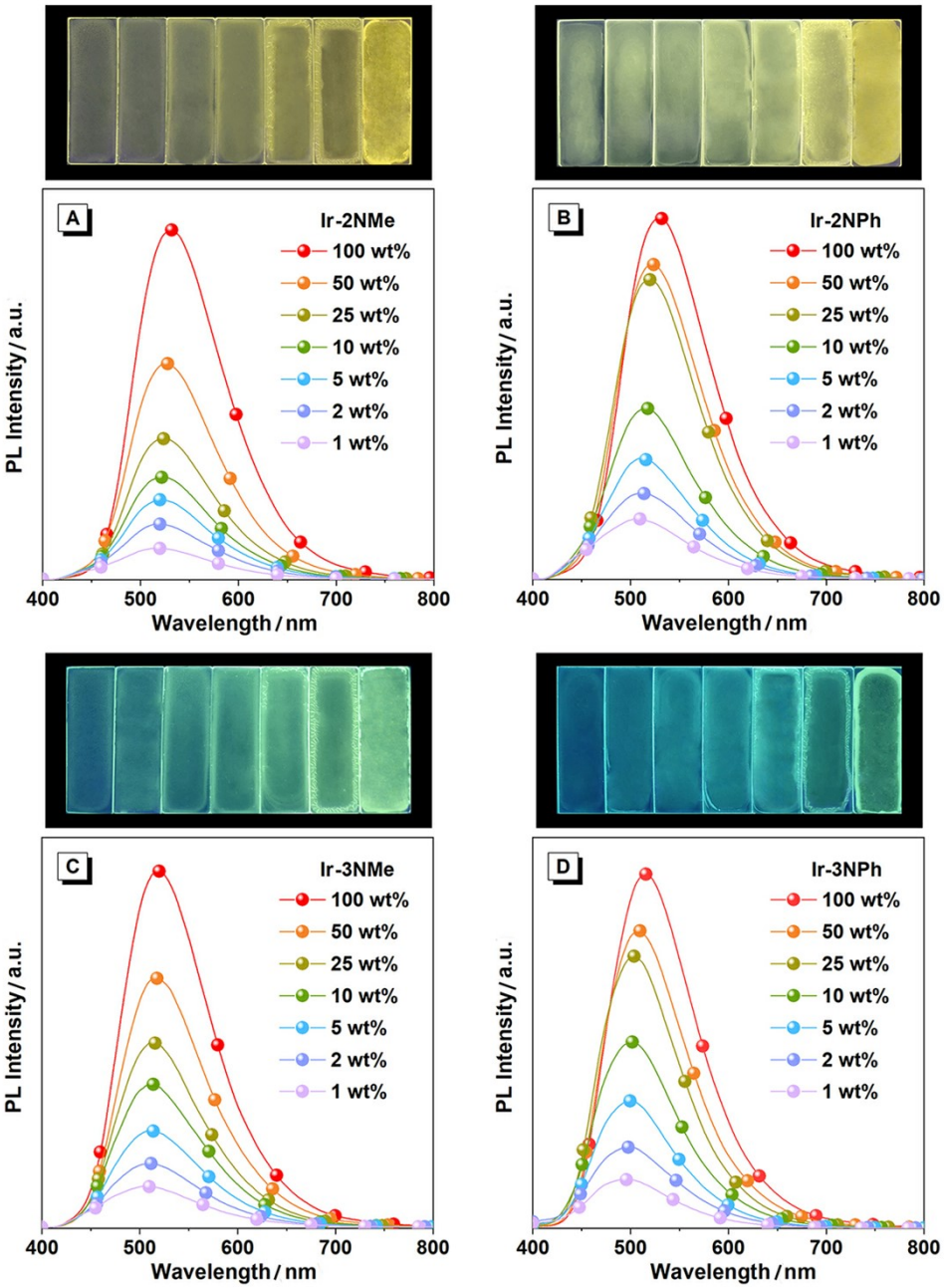

Fig. **S20** Photoluminescence spectra and luminescent photographs of complexes (A) **Ir-2NMe**, (B) **Ir-2NPh**, (C) **Ir-3NMe**, and (D) **Ir-3NPh** in doped films (1-100 wt% doping concentration, PMMA as the host).

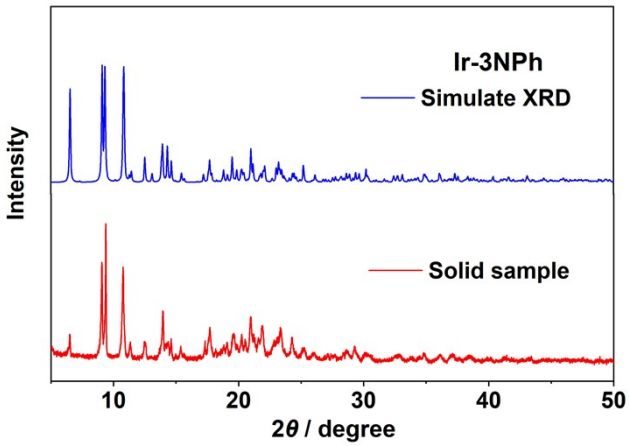

Fig. **S21** XRD diffractograms of solids and XRD diffractograms simulated from crystal structures for complex **Ir-3NPh**.

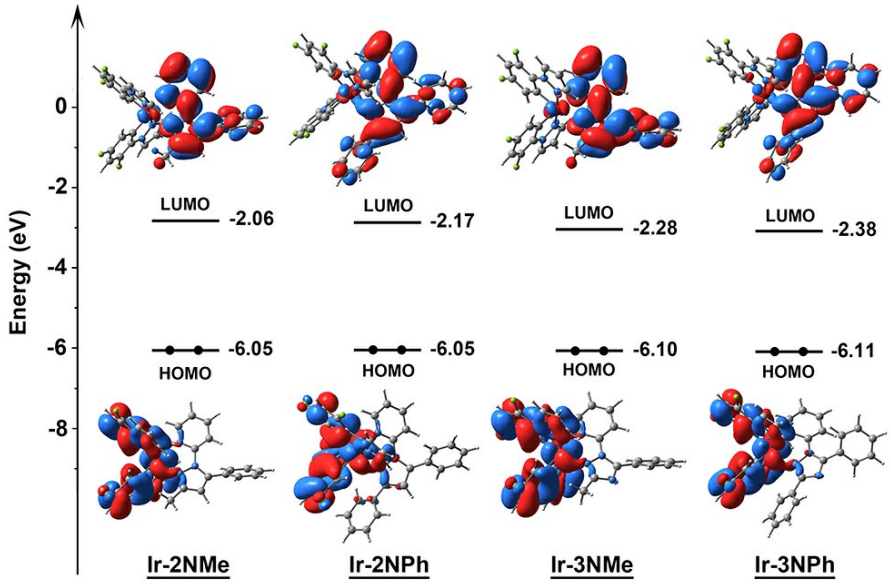

Fig. **S22** Electronic levels and surface distributions of HOMO and LUMO orbitals for four complexes.

Table S4 The calculated energy levels of the lower-lying transitions of complexes **Ir-2NMe**, **Ir-2NPh**, **Ir-3NMe**, and **Ir-3NPh**.

Complexes	States	Assignment	eV	Nature
Ir-2NMe	T_1	H-1→L (34%) H→L (56%)	1.71	MLCT/LLCT/LC MLCT/LLCT/LC
Ir-2NPh	T_1	H-1→L (48%) H→L (41%)	1.79	MLCT/LLCT/LC MLCT/LLCT/LC
Ir-3NMe	T_1	H-1→L (76%) H→L (11%)	1.74	MLCT/LLCT/LC MLCT/LLCT
Ir-3NPh	T_1	H-1→L (54%) H→L (33%)	1.87	MLCT/LLCT/LC MLCT/LLCT/LC
Ir-Y3NMe	T_1	H→L (98%)	2.27	MLCT/LLCT
Ir-Y3NPh	T_1	H→L (93%)	2.19	MLCT/LLCT

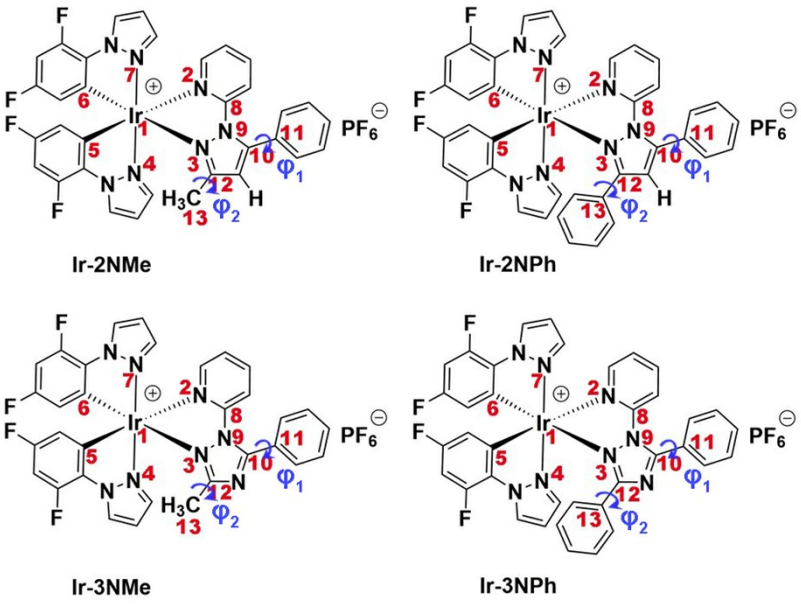

Table S5 The bond lengths (Å), bond angles (°) and dihedral angles (°) modifications

from S_0 to T_1 as calculated by DFT approach for complexes **Ir-2NMe** and **Ir-2NPh**.

Ir-2NMe			**Ir-2NPh**		
Bond lengths (Å)	S_0	T_1	Bond lengths (Å)	S_0	T_1
Ir1-N2	2.204	2.197	Ir1-N2	2.203	2.201
Ir1-N3	2.202	2.126	Ir1-N3	2.250	2.151
Ir1-N4	2.053	2.047	Ir1-N4	2.051	2.045
Ir1-C5	2.030	2.036	Ir1-C5	2.030	2.034
Ir1-C6	2.026	2.038	Ir1-C6	2.020	2.035
Ir1-N7	2.049	2.058	Ir1-N7	2.055	2.061
C10-C11	1.476	1.406	C10-C11	1.475	1.408
C12-C13	1.494	1.491	C12-C13	1.472	1.470
Bond angle (°)	S_0	T_1	Bond angle (°)	S_0	T_1
N2-Ir1-N7	74.2	75.4	N2-Ir1-N7	74.0	75.0
N4-Ir1-C5	79.9	79.9	N4-Ir1-C5	79.8	79.8
N7-Ir1-C6	79.9	79.5	N7-Ir1-C6	79.9	79.7
Dihedral angles (°)	S_0	T_1	Dihedral angles (°)	S_0	T_1
φ_1	54.1	27.5	φ_1	52.6	24.8
φ_2	--	--	φ_2	42.8	46.2

Table S6 The bond lengths (Å), bond angles (°) and dihedral angles (°) modifications from S_0 to T_1 as calculated by DFT approach for complexes **Ir-3NMe**, and **Ir-3NPh**.

Ir-3NMe			**Ir-3NPh**		
Bond lengths (Å)	S_0	T_1	Bond lengths (Å)	S_0	T_1
Ir1-N2	2.213	2.202	Ir1-N2	2.211	2.201
Ir1-N3	2.203	2.126	Ir1-N3	2.257	2.177
Ir1-N4	2.053	2.046	Ir1-N4	2.053	2.045
Ir1-C5	2.029	2.035	Ir1-C5	2.029	2.033
Ir1-C6	2.024	2.037	Ir1-C6	2.019	2.031

Ir1-N7	2.050	2.061	Ir1-N7	2.057	2.062
C10-C11	1.472	1.406	C10-C11	1.471	1.419
C12-C13	1.489	1.486	C12-C13	1.468	1.451
Bond angle (°)			Bond angle (°)		
N2-Ir1-N3	74.2	75.1	N2-Ir1-N7	74.1	74.7
N4-Ir1-C5	79.9	79.9	N4-Ir1-C5	79.8	79.8
N7-Ir1-C6	80.0	79.5	N7-Ir1-C6	79.9	79.7
Dihedral angles (°)			Dihedral angles (°)		
φ_1	47.6	25.7	φ_1	45.6	23.2
φ_2	--	--	φ_2	35.4	24.7

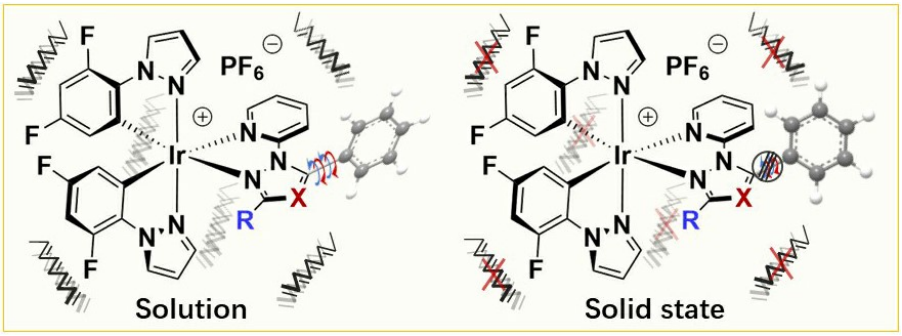

Fig. **S23** Conceptual diagram of the motion simulation of complexes **Ir-2NMe**, **Ir-2NPh**, **Ir-3NMe**, and **Ir-3NPh** in solution and solid state.

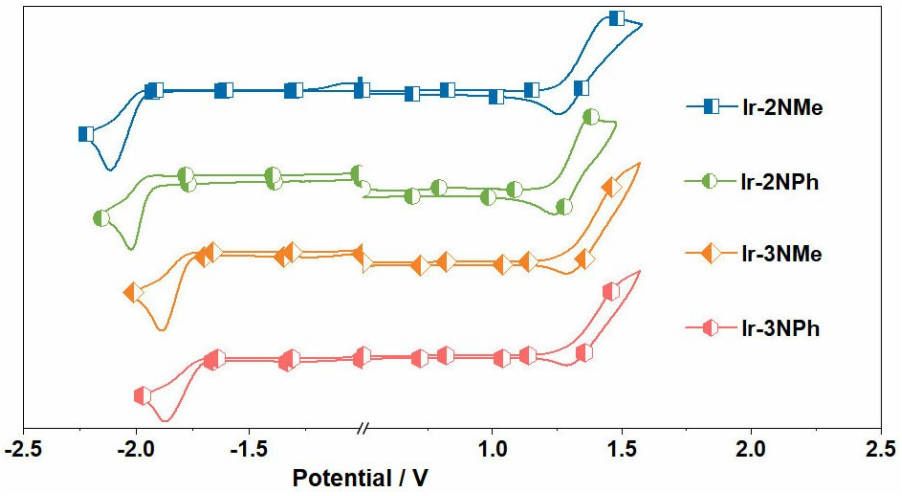

Fig. **S24** Cyclic voltammograms of complexes **Ir-2NMe**, **Ir-2NPh**, **Ir-3NMe**, and **Ir-3NPh** in degassed CH_3CN solution with 0.1 M $TBAPF_6$ as electrolyte (scan rate = 100 mV/s).

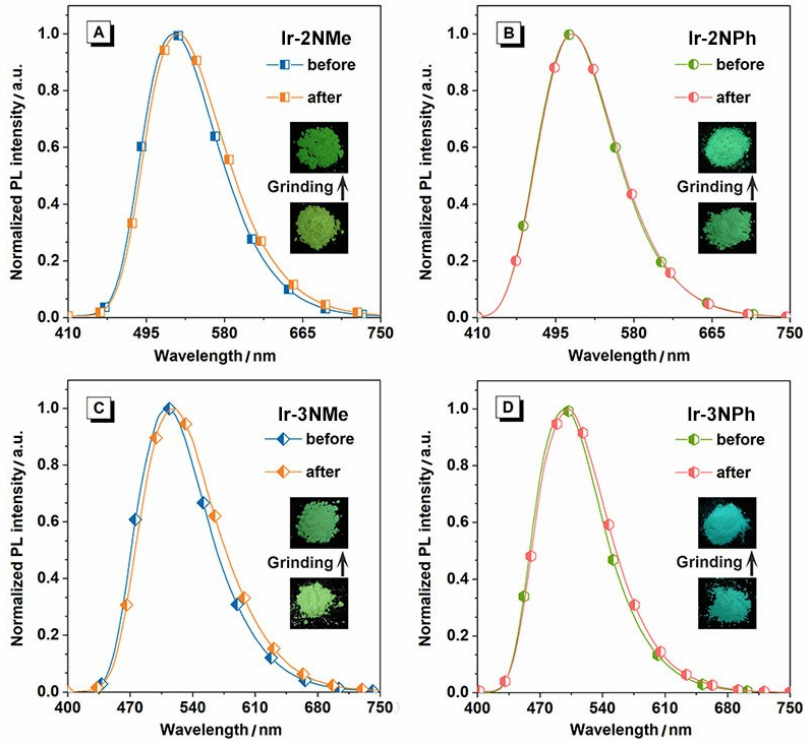

Fig. **S25** Emission spectra of complexes (A) **Ir-2NMe**, (B) **Ir-2NPh**, (C) **Ir-3NMe**, and (D) **Ir-3NPh** before and after grinding.

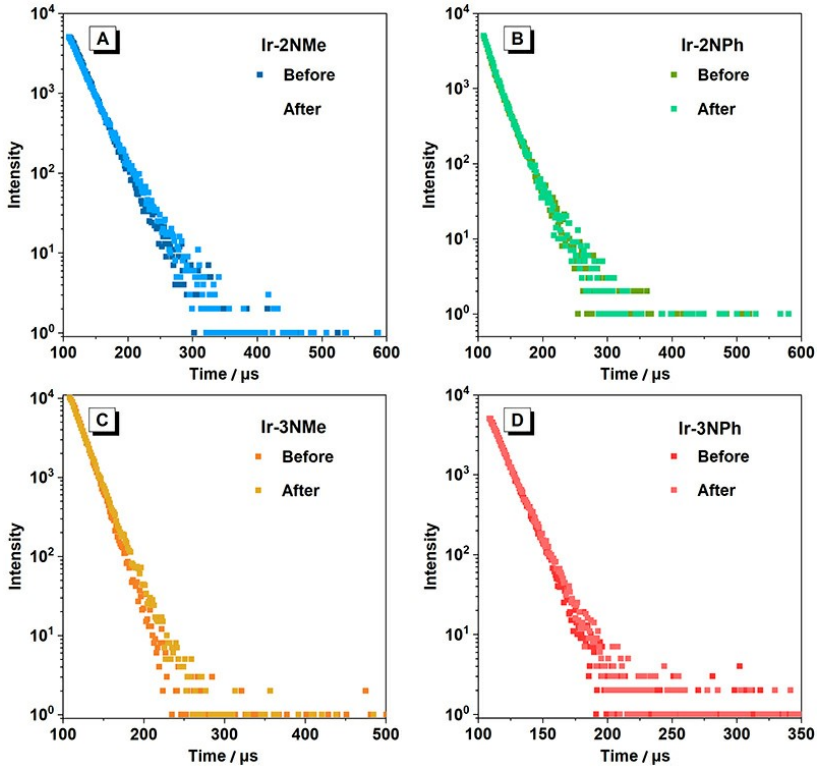

Fig. **S26** Emission lifetime decay curves for complexes (A) **Ir-2NMe**, (B) **Ir-2NPh**, (C) **Ir-3NMe**, and (D) **Ir-3NPh** before and after grinding.

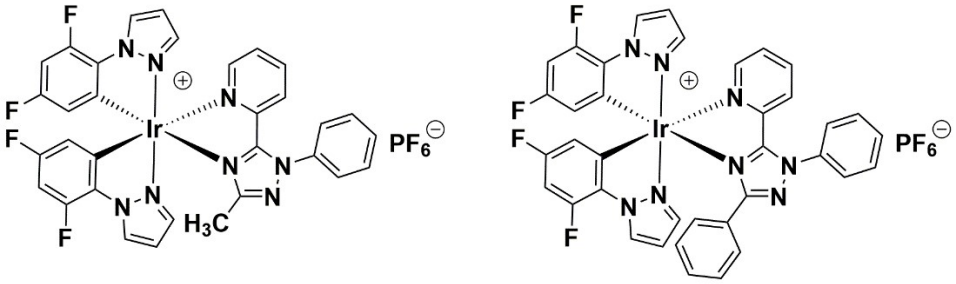

Fig. **S27** Chemical structures of the complex **Ir-Y3NMe** and **Ir-Y3NPh**.

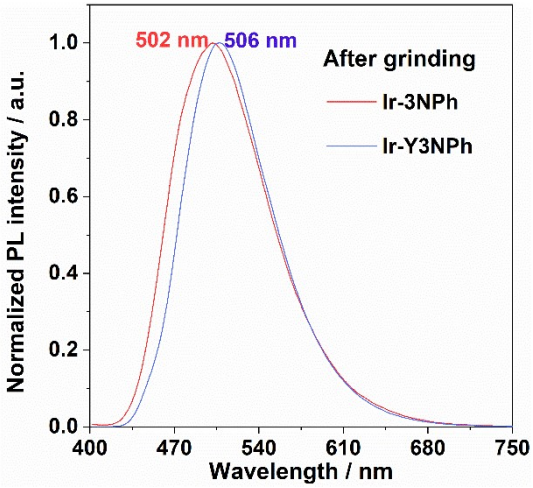

Fig. **S28** Emission spectra of complexes **Ir-3NPh** and **Ir-Y3NPh** after grinding.